Energy Response, IR Attenuation and AGN Sensitivity

Elizabeth Hays

June 19, 2003

1 Intro

While working on the flux limits for the Costamante and Ghisellini AGN, I wanted to understand at what energy the flux limits should be quoted. In general for the flux normalization ≈ 4 TeV is a great spot for straight power laws while the median energy is a better place for IR attenuated spectra. Quoting above the median energy for integral fluxes still seems reasonable when accompanied by the appropriate caveats.

I have also been thinking about ways to talk about flare sensitivity in general. The result is a loose collection of plots on energy response and sensitivity. I consider the effects of declination, spectral index, flare duration, and IR attenuation on Milagro observations. If an arbitrary horizon is defined as the redshift where a source needs more than 10 times the Crab flux for a 5σ detection, for 1 year $z = 0.1$ and for 1 month $z = 0.04$. Additionally redshift narrows the field of view. The same sensitivity threshold at $\pm 30°$ from overhead for $z = 0.02$ is at $\pm 15°$ at $z = 0.10$ for a 5σ/year detection.

I describe in no detail how I turn the simulations into fluxes since that is another memo in progress. The Monte Carlo data cuts are the same throughout the memo: pmt count > 55, delangle < 1.2 and X2 > 2.5 with radial and cos(theta) weights, spectral reweighting as necessary and a reasonable set of dead tubes. Flux results include 94% electronic deadtime and do not include corrections for the point spread function. I do describe the IR models I use and give references for them. Hopefully this study will shed some light on how Milagro's sensitivity to AGN relates to redshift, spectral index and declination.

2 Simple Power Law Spectra

First, I have to deal with the basics. Before considering attenuation effects I ask what energy best applies to AGN observations assuming a simple power law. AGN spectra at TeV energies are fairly well measured for a few sources. However, these sources have been observed to change spectral index with flux level and time-averaged spectra are known to change from year to year. The time average from ACTs is only known for some hundred or so hours a year at the best.

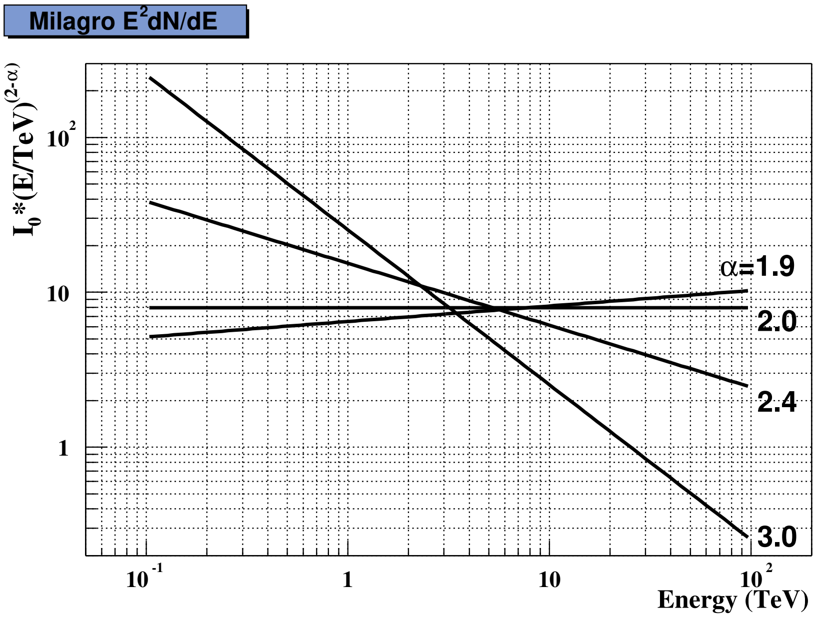

Figure 1: $E^2 dN/dE$ as a function of energy, where $dN/dE = I_0 E^{-\alpha}$. I_0, the flux normalization, is calculated from Monte Carlo data using a fixed Milagro event rate and applying different spectral indexes. The region where the lines intersect indicates where the differential flux normalization is least dependent on choice of spectrum. The center of this region is 4.3 ± 1.4 TeV.

Milagro flux measurements and limits are affected by the spectrum used in the area calculation. For well-known AGN we get a lightly sampled average for the spectral index from ACTs while for predicted emitters like the Costamante AGN the index is an educated guess using lower energy data. In the case of a Milagro discovery we could use the TeV spectral average, but then again it should probably be the average for high flux flares which is different. Of course, when an energy cut off is included, the index changes again. For example, Hegra's time averaged index for Mrk 421 in Nov 2000 - May 2001 goes from 3.05 to 2.19 when an energy cut off is included in the fit

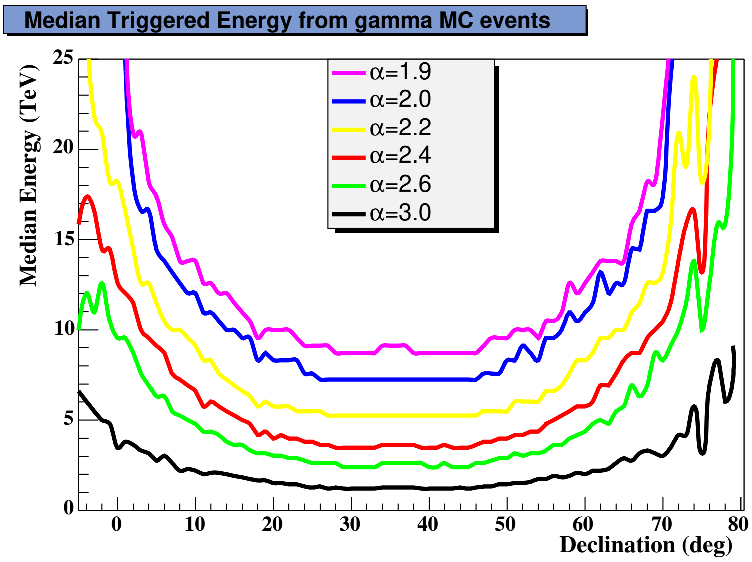

Figure 2: Median triggered energy for an $E^{-\alpha}$ spectrum as a function of declination. At declinations $\pm 10°$ from overhead the energy response is quite flat. Past $\pm 25°$ to $\pm 30°$ response becomes steep for most spectra where only high energy photons produce triggers.

(A&A 393 89A, 2002). In Milagro this translates to a 22% difference in the flux normalization. My point is that the error in spectral index can be large and we should try to minimize the impact it has on our limits. It would be helpful to be able to quote a flux normalization at an energy where the result is least affected by the spectrum we choose.

To look at sensitivity to changes in spectral index, I plot $E^2 dN/dE$, where $dN/dE = I_0 E^{-\alpha}$, against energy. I pick an arbitrary event rate in the detector and calculate the flux normalization, I_0, using the effective area for some spectral index, α. I use this I_0 in the dN/dE equation and plot $E^2 dN/dE$ from 100 GeV to 100 TeV. For a set of indexes the region in energy in the $E^2 dN/dE$ plot where the lines intersect shows where the flux normalization is most spectrally independent. By defining the center as the mean of the energies of the crossings I get 4.3 ± 1.4 TeV (fig 1). This energy is a stable place to quote AGN flux normalizations. In addition, it falls near the middle of the range of median triggered energy for the same set of spectral indexes (fig 2) and agrees with the median energy in the Crab paper.

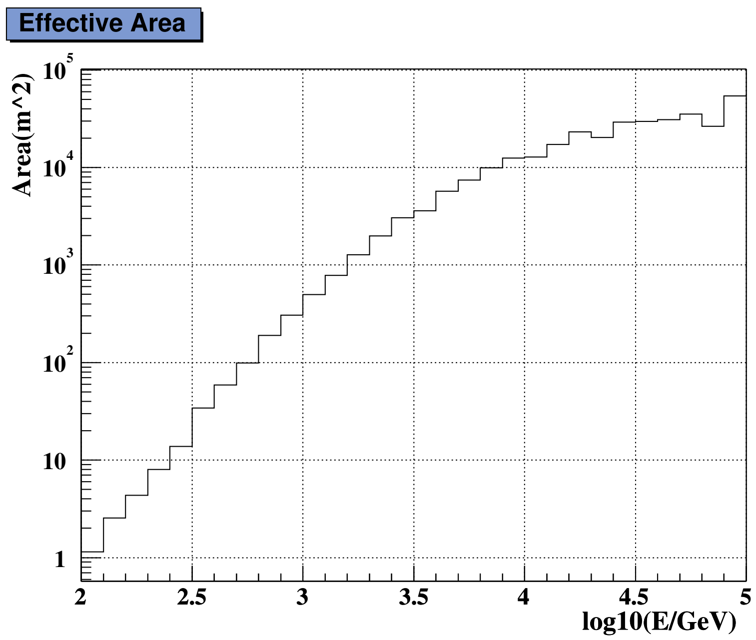

Figure 3: Effective area in m^2 as a function of energy for reference.

3 Infrared Background Attenuation

For extragalactic TeV observations absorption effects must be considered beacuse infrared background light from stars and dust re-radiation causes pair production with TeV photons. TeV observations of blazars by ACTs provide evidence for spectral energy cut offs of a few TeV (see papers on MKN 421, MKN 501,H1426+428 spectra by Whipple or Hegra and most recently 1ES1959+650 by Hegra). To say something about our DC and flaring sensitivity to AGN some sort of redshift attenuation effect should be included.

Attenuation effects can instead be included as an energy cut off, where $dN/dE = I_0 E^{-\alpha} e^{E/E_c}$, which has no explicit dependence on redshift and can include attenuation effects other than from the IR background. However, I don't show any results for simple cut off energies in this memo. Using the models may be less accurate but more instructive than just including a cut off because it gives some feel for a reasonable range of sensitivity as a function of redshift.

3.1 Infrared Background Models

To include IR attenuation effects I use two types of models. One is an extrapolation of Malkan and Stecker (2001, ApJ 555,641) by Stecker and

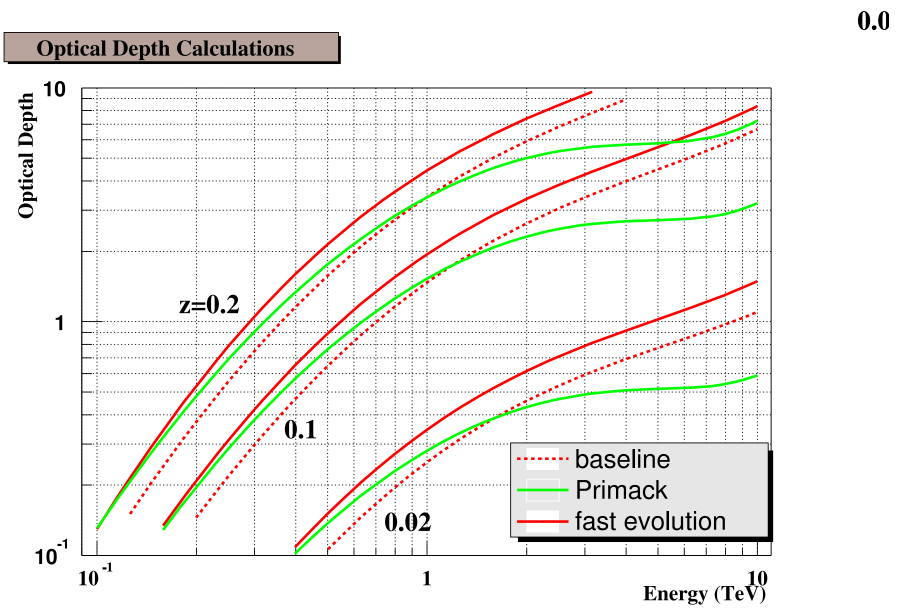

Figure 4: Optical depth calculations used to apply a redshift dependence to the energy spectrum. The two types of models differ most at low redshift where for the most part $\tau < 1$ in Milagro's energy range.

de Jager (2002, ApJ, 566, 738) and has two variations - baseline and fast evolution star formation models. I'll refer to the baseline model as S&J 1 and the fast evolution model as S&J 2. I also use a semi-analytic model by Somerville and Primack for LCDM cosmology with functional fits given in James Bullock's thesis (UCSC 1999). I'll refer to this model as S&P and append the formula and coefficients (Appendix A).

Both models parameterize the optical depth of the universe as a function of redshift and energy. The Stecker and Primack models predict slightly different present-day energy densities at IR frequencies with Stecker's model predicting higher energy density in the mid-IR. In general S&J 2 predicts the most attenuation and S&P the least in Milagro's energy range although this breaks down a bit at high redshifts (fig 4). At high redshift, S&J 1 and S&P have similar effects on our detector response although the shape of $\tau(E)$ differs.

3.2 Comments on Models

The predicted attenuation is applied to a power law spectrum in the following way, $dN/dE = I_0 E^{-\alpha} e^{-\tau(E,z)}$, where τ is the optical depth. This has a strong effect on effective areas and triggered energy distributions (fig 5, fig 6). Note that at high redshift where the area is small, there is some error

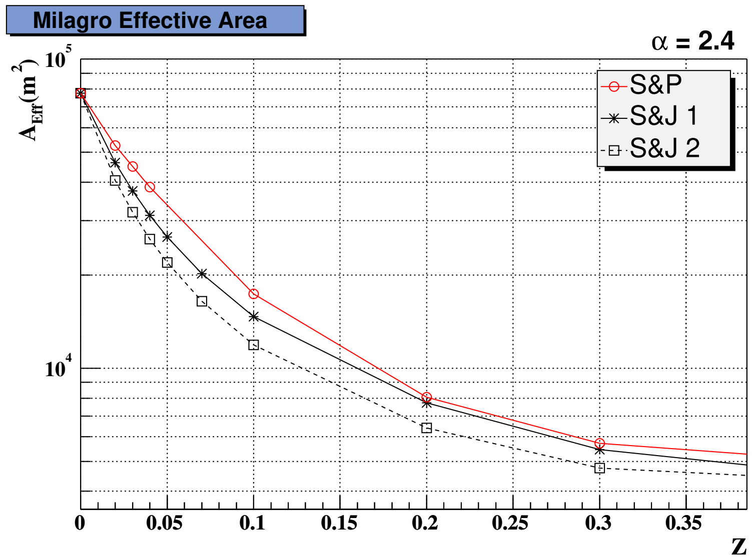

Figure 5: Effective area as a function of redshift for an $E^{-2.4}$ spectrum. The areas for S&J 1 and S&P almost converge at high redshifts where the models differ most at energies that are highly attenuated and fail to produce triggers.

in area and median energy because I have not included MC data for the low energy band 50-100 GeV. This only becomes important when the area below 100 GeV is not a negligible fraction of the total area. I do plan to include the low energy Monte Carlo data in future studies.

Stecker and de Jager give the redshift bounds of their parameterization as $0.03 < z < 0.3$. Milagro areas that result from using redshifts below 0.03 are consistent with interpolating the area between $z = 0$ and $z = 0.03$. The area using this model may be overly conservative for this region but it is not unreasonable. The area for $z > 0.3$ out to $z = 0.5$ converges for the two Stecker models so there is probably some growing error in the extrapolation. However, the values are not unreasonable.

The parameterization for the Primack model is given coarsely in redshift for the values shown in table 1 (also see Appendix A). In this memo results for this model are only for those exact redshift coefficients. However, flux results could be interpolated between the given values for sources with known redshift. Because the Primack fit is not given as a function of redshift and S&J 1 falls in the middle of the models in terms of optical depth, I make S&J 1 the default model. Results can be interpreted as becoming slightly better or worse depending on which model you prefer. I will show some results for the other models to put a range on how much each affects sensitivity.

Redshift	S & J 1		S & J 2		S & P	LCDM
	$A_{eff}(m^2)$	E_c(TeV)	A_{eff}	E_c(TeV)	A_{eff}	E_c(TeV)
0	77454	—	77454	—	77454	—
0.02	46173	8.9	40484	4.5	52537	17.8
0.03	37445	3.5	31958	2.2	44889	11.2
0.04	31208	2.2	26145	1.4	38508	3.5
0.05	26563	1.4	21967	1.1	—	—
0.07	20212	1.1	16470	0.6	—	—
0.1	14688	0.7	11898	0.5	17392	0.7
0.2	7721	0.4	6409	0.3	8055	0.4
0.3	5461	0.2	4759	0.2	5714	0.2
0.5	4151	0.1	3000	0.1	4738	0.1

Table 1: Effective area for $0.1 < E < 100$ TeV is given for various redshifts. A_{eff} decreases with redshift but even at $z = 0.3$ the area is >5000 m^2 for an $E^{-2.4}$ spectrum. The cutoff energy is given for each redshift and model with E_c defined as the energy where $\tau = 1$.

4 Running the Numbers

4.1 Energy and Area

I begin by exploring the effects of attenuation on effective area and median energy. The effective area values for S&J 1 and S&P are included in table 1. For reference I have included a plot of effective area as a function of energy (fig 1). Median triggered energy is highly correlated with effective area and tracks the high energy cutoff (fig 6). Both can be considered functions of a cutoff energy so I have included those conversions (see table 1). I interpreted the cutoff energy for the models as the energy where $\tau = 1$. Note that the cutoff energy for S&J 1 at $z = 0.03$ is quite close to the 3.6 TeV, the cutoff energy Hegra fit to MRK 421 data ($z = 0.031$) for Dec. 1999-2001.

To look at the effects of increasing redshift on median energy, I show median energy as a function of declination for several redshifts using S&J 1. The median energy curve flattens in declination with increasing redshift. For the $z = 0$ median energy plot the flat region also indicates where in declination Milagro is sensitive. In this case the flattening indicates the loss of higher energy triggers which are the bulk of the triggers at high declination. The sensitivity at those declinations for $z > 0$ is actually quite low (fig 8).

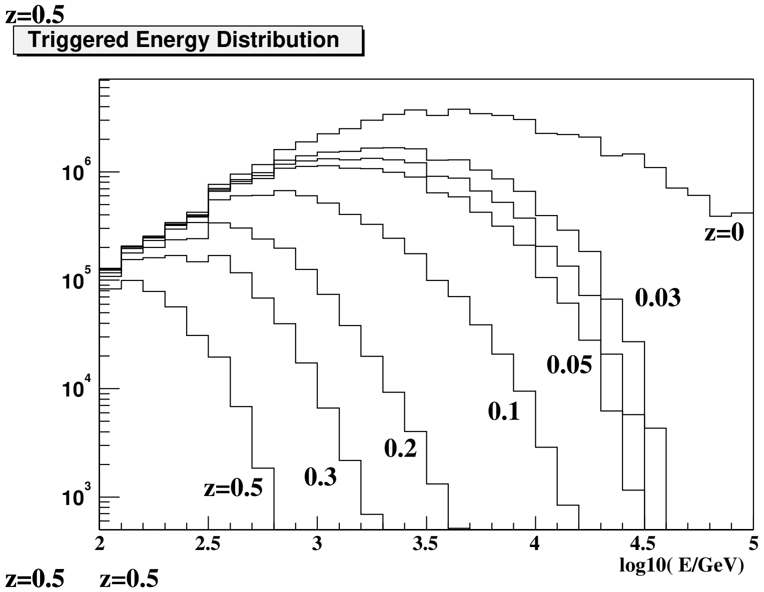

Figure 6: Evolution of the triggered energy distribution with redshift for an $E^{-2.4}$ spectrum. Attenuation is calculated using S&J 1.

4.2 DC Sensitivity

For the DC source I choose a Crablike object with an $E^{-2.59}$ spectrum. I put this hypothetical source at some redshift by adding attenuation and ask what flux normalization is required for a detection at 5σ in a year. From data I get a live time of 91% so I use 1 year = 332.5 days of exposure. Because Milagro's sensitivity changes with declination, I consider several when looking at redshift effects. Using the background levels from data I find event rates required for a 5 sigma excess at 36°,26°, 21°,and 6° declination, which are respectively 0°,−10°,−15°, and −30° from overhead. I show the flux results for redshift using several declinations (fig 9) and for declination using several redshifts (fig 8). Note that +10°,+15°, and +30° from overhead are not symmetric (figure 8 is not centered on Milagro's latitude) due to longer daily exposures for sources transiting north of Milagro.

For figure 9 I assume a Crablike spectrum. Something in a long term flaring state would likely have a flatter spectrum and require less flux. However, the general trends remain the same. As redshift increases we lose sensitivity, especially far from zenith. At $z = 0.05$ a source flux need only be a 5-6 times the Crab flux but that only applies within $\pm 10 - 15°$ from zenith. Much past $z = 0.1$ the source flux must be greater than 10 times the Crab flux and transit near zenith. In figure 9 we see that the sensitivity curves for declinations further from zenith diverge. Effectively we get a narrower field of view with increasing redshift.

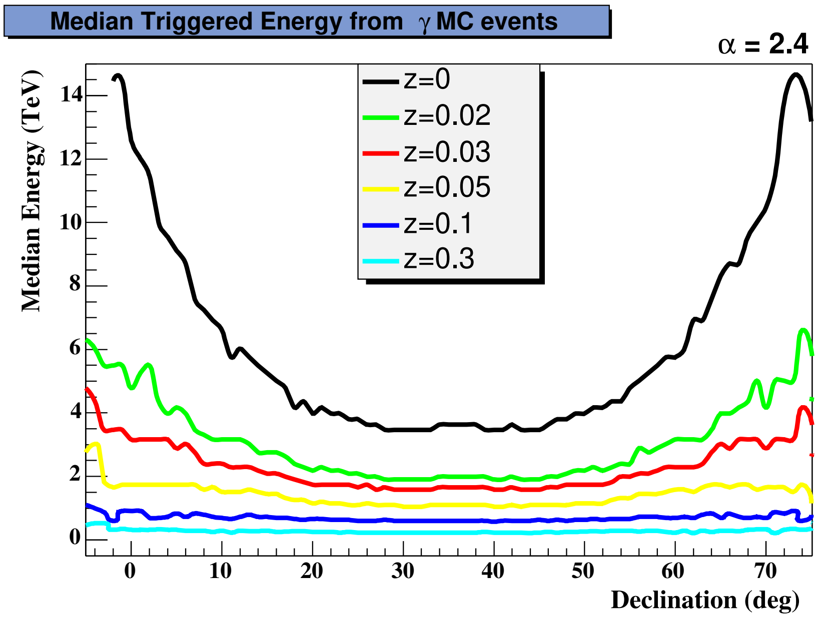

Figure 7: Median energy for $E^{-2.4}e^{-\tau(E,z)}$ falls below that selected as spectrally independent in figure 1. The energy flattens in declination with redshift, but a look at sensitivity (fig 8) shows that as redshift increases the sensitivity drops at high declinations where photons that trigger must have high enough energy to penetrate a thicker cut of atmosphere.

4.3 Flaring Sensitivity

The flaring example is very similar to the DC example. I require 5σ in a detector month, 30 days $\approx$ 27.3 days of exposure, using background levels from data. The results shown are for an $E^{-2.2}$ spectrum because it is near the time-averaged flare spectrum for Mrk 421. For comparison I include an $E^{-2.4}$ spectrum at 36° and also the results for S&P IR attenuation. In general we do slightly better for S&P IR and slightly worse for S&J 2. I have mostly shown results for S&J 1 since it is in the middle at low redshift.

Just as in the DC case the field of view narrows with redshift. The spectrum is flatter than the DC example which allows a more optimistic flux requirement for the less absorptive S&P model. To balance things out I also include the more pessimistic (though not by much) $E^{-2.4}$ spectrum. Notice that the underlying power law makes less of a difference as the redshift cutoff moves lower in energy. A month is not an unreasonable time scale for us to see a flaring AGN, but it had better be bright, close, and not much more than 15° from zenith. Flaring on timescales of a few months limits the horizon to around redshifts of 0.04 to 0.05.

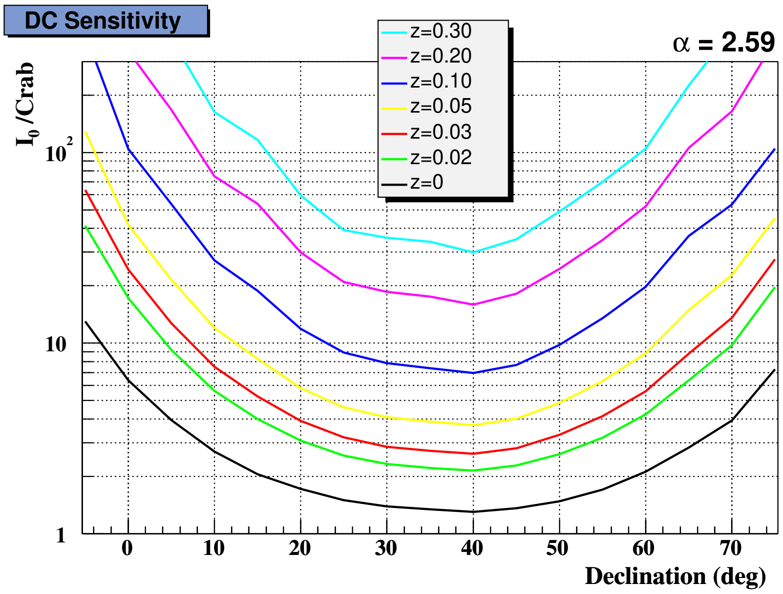

Figure 8: The flux normalization in Crab units required to get a 5σ/yr excess for a source at a given redshift as a function of declination. 1 year = 332.5 days of exposure. The spectrum is $E^{-2.59}e^{-\tau}$ with S&J 1 attenuation.

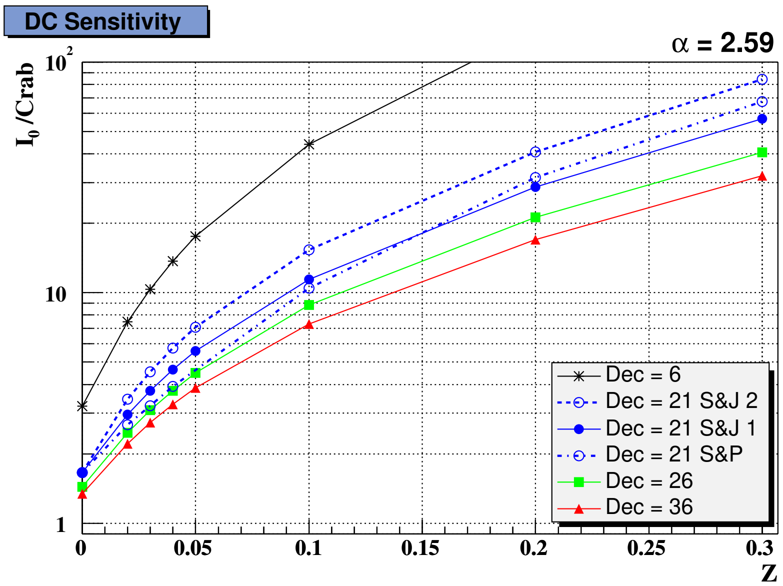

Figure 9: The flux normalization in Crab units required for a 5σ/yr detection for S&J 1 using $dN/dE = E^{-2.59}e^{-\tau}$ at several declinations. At 26° DEC the flux ratio is shown using S&J 2 and S&P for comparison.

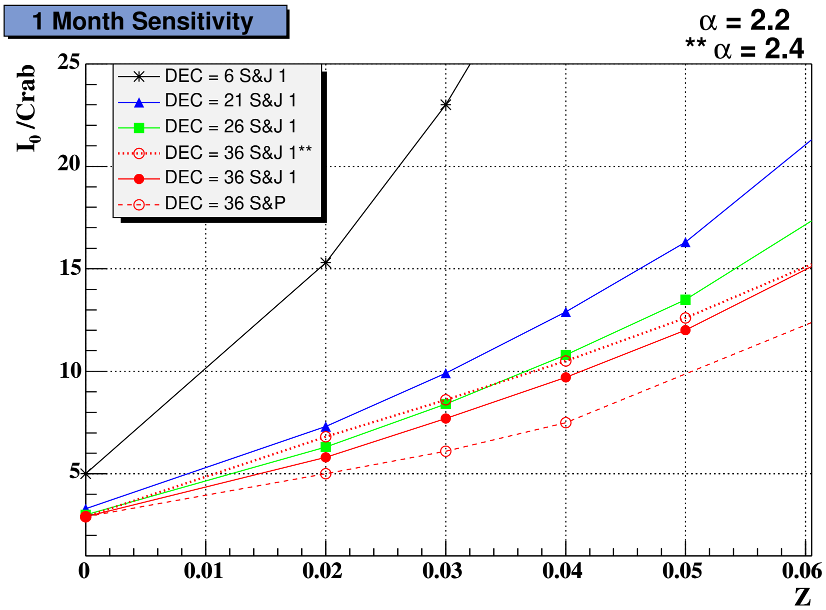

Figure 10: The flux normalization in Crab units required to get a 5σ/month excess is calculated for a source at 6°, 21°, 26° and 36° DEC with $dN/dE = E^{-2.2}e^{-\tau}$ and S&J 1 attenuation. One month = 27.3 days of exposure. At 36° results are shown for an $E^{-2.4}$ spectrum and also for S&P IR.

5 Conclusions

I already talked about the results in the intro so I guess this is the place to philosophize? I had a hope that beyond figuring out how to talk about sensitivity in the first place I could find one plot to define Milagro's AGN sensitivity. Here I conclude this does not work. Spectral shape, which now has two components, and declination both have strong and interrelated effects on sensitivity. Because of Milagro's energy response, one has to be taken in the context of the other. Median energy is important, but not without understanding what is due to the spectrum, what is due to the detector and whether there is any sensitivity. On the other hand, I think most of this will be quite useful when applied to specific sources. Given a specific declination and redshift, which can be treated as some sensible cutoff or model with bounds, only the underlying power law index is left dangling. All that remains is to actually apply this to some real sources. And so to the next memo.

A S&P IR Model

The following is taken from chapter 9, pp 142,146, of James Bullock's thesis from UCSC. The functions match the models to within 5% for $0.01 < \tau < 10$ and $0.1 < E < 100$ TeV.

$$\tau(E) = \tau_1(E) + \tau_2(E) \tag{1}$$

where

$$\tau_1(E) = \tau_1 \exp[-(\frac{\log_{10}(E/E_1)}{\Delta_1})^2] \tag{2}$$

$$\tau_2(E) = \tau_1 \exp[-(\frac{\log_{10}(E/E_2)}{\Delta_2})^4] \tag{3}$$

z_s	τ_1	$\log_{10} E_1$	Δ_1	τ_2	$\log_{10} E_2$	Δ_2
0.02	0.49	12.59	0.79	12586.52	20.70	4.23
0.03	0.74	12.59	0.79	19212.86	20.64	4.19
0.04	0.99	12.58	0.79	20930.67	20.58	4.18
0.10	2.63	12.59	0.80	226.28	16.36	2.22
0.20	5.59	12.57	0.81	71.17	15.16	1.62
0.30	8.96	12.55	0.82	507.96	15.35	1.64
0.50	0.96	11.47	0.57	15.39	13.03	1.35
1.00	66.27	12.71	0.95	0.00	1.00	1.00

Table 2: Fit parameters for Somerville and Primack optical depth using LCDM cosmology as defined in equations 1,2 and 3. Symbol z_s refers to the source redshift. Energies E_1 and E_2 are in units of eV.